Comparison of fluorescence tomographic imaging in mice with early-arriving and quasi-continuous-wave photons

Mark Niedre[1,3] and Vasilis Ntziachristos[2,3,*]

[1]*Department of Electrical and Computer Engineering, Northeastern University, Boston, Massachusetts 02115, USA*
[2]*Institute for Biological and Medical Imaging, Technical University of Munich and Helmholtz Center Munich, Ismaningerstrasse 21, D-85764 Munich, Germany*
[3]*Laboratory for Biooptics and Molecular Imaging, Center for Molecular Imaging Research, Massachusetts General Hospital and Harvard Medical School, Charlestown, Massachusetts 02129, USA*
**Corresponding author: v.ntziachristos@tum.de*

Received October 2, 2009; revised November 20, 2009; accepted November 21, 2009; posted December 23, 2009 (Doc. ID 118123); published January 27, 2010

The highly diffuse nature of light propagation in biological tissue is a major challenge for obtaining high-fidelity fluorescence tomographic images. In this work we investigated the use of time-gated detection of early-arriving photons for reducing the effects of light scatter in mice relative to quasi-cw photons. When analyzing sinographic representations of the measured data, it was determined that early photons allowed a reduction in the measured FWHM of fluorescent targets by a factor of approximately 2–3, yielding a significant improvement in the tomographic image reconstruction quality. © 2010 Optical Society of America

OCIS codes: 110.6955, 170.6920, 300.2530.

Fluorescence molecular tomography (FMT) is an emerging small animal imaging technique that allows visualization of three-dimensional distributions of fluorescent bio-markers *in vivo* [1,2]. In spite of marked advances in instrumentation and image reconstruction approaches in recent years, FMT remains limited by the high degree of light scatter in tissue, which results in a highly ill-posed image reconstruction problem versus, for example, x-ray computed tomography (CT) [3]. Time gating of detected photon fields has been proposed by several groups as a method to minimize the effects of light scatter by preferentially selecting "early-arriving" photons that propagate along more direct paths between source and detector pairs [4–7]. As discussed by LeBlond *et al.* [7], the measurement of early photons allows improved imaging resolution, since it allows the retention of imaging singular modes corresponding to higher spatial frequencies in the image reconstruction problem. Recently, we demonstrated the use of early photons for fluorescence tomographic imaging of Lewis lung carcinoma-bearing mice [8].

In this work we investigated the improvement obtained with early photons versus later-arriving diffuse photons in mice, specifically, euthanized mice with implanted fluorescent tubes in the torso. This allowed us to observe the improvement obtained by temporal gating of detected photon fields without factors such as the bio-distribution and pharmacokinetics of injected fluorescent probes (which can complicate the interpretation of results) while maintaining experimental realism—such as tissue optical heterogeneity and autofluorescence [9,10]—that cannot be easily approximated using optical phantoms [11]. Herein, we demonstrate that when transmitted through the torso of a mouse, early photons were significantly less diffuse than quasi-cw photons and allowed an improved visualization of fluorescent targets for individual optical projections and reconstructed tomographic images. To our knowledge this has not been demonstrated previously in mice.

The instrument used in these experiments is shown in Fig. 1 and was described in detail previously [8]. Mice were placed in a carbon-fiber tube that was suspended in the 2.2-cm-wide imaging chamber and the transmitted light was imaged with a high-speed gated intensified CCD (ICCD) (LaVision Picostar, Lavision, Ypsilanti, MI). Female nu/nu mice (COX7, Massachusetts General Hospital, Boston, MA) were first euthanized with carbon dioxide asphyxiation. Two 1 mm internal-diameter semi-transparent tubes containing 750 nM Alexafluor-750 were implanted in the torso of the animal—in an approximately parallel orientation with the first (1 cm in length) placed subcutaneously outside the ribcage and the second (5 cm in length) inserted in the esophagus [12]. This resulted in a background autofluorescence contrast ratio of approximately 10:1.

The 2.2 cm imaging chamber was filled with a liquid solution with optical properties matching that of the mouse thoracic cavity [10] at 730 nm—$\mu_s' = 25\ \mathrm{cm}^{-1}$, $\mu_a = 0.3\ \mathrm{cm}^{-1}$—prepared from a stock solu-

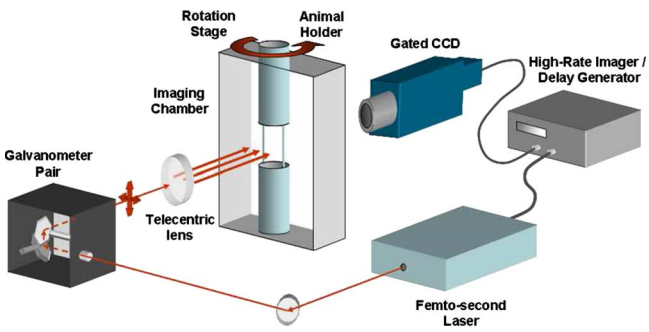

Fig. 1. (Color online) Fluorescence tomographic imaging system used in these experiments. Early-arriving and quasi-cw photons from the pulsed femtosecond laser were detected with the gated ICCD.

tion of 10% Intralipid (Baxter Healthcare) and ink (Higgins Ink, Sanford). Mice were rotated over 360° in 5° increments so that single axial slices of the animal were scanned with a row of 45 beam positions separated by 0.5 mm for each angle. Images were taken of early and quasi-cw photons at the excitation and fluorescence wavelengths with gating parameters relative to the laser pulse as follows: (i) early excitation: width=200 ps, center=200 ps; (ii) early fluorescent: width=200 ps, center=250 ps; (iii) quasi-cw excitation: width=1000 ps, center=550 ps; and (iv) quasi-cw fluorescent: width=1000 ps, center=900 ps. Since the maximum temporal gate width of the ICCD was 1000 ps, conditions (iii) and (iv) were intended to approximate the cw case. With these parameters, the system signal-to-noise ratio was on average 23 dB for early photons and 28 dB for quasi-cw photons, reflecting the noise trade-off of the technique.

ICCD images were analyzed to yield sinograms of the transmitted fluorescence intensity normalized to the transmitted excitation intensity as a function of the lateral position and rotation angle for early and quasi-cw photons as shown in Figs. 2(a) and 2(b). This normalization operation virtually cancels any effect of tissue optical heterogeneity in the animal [13]. A standard "rebinning" routine was used to calculate the transmitted intensity profile at angles in 1° increments; this was done by including pixels in the analysis up to ±2.5° (equivalent to 1 mm) off-axis from the pixel directly opposite the source position,

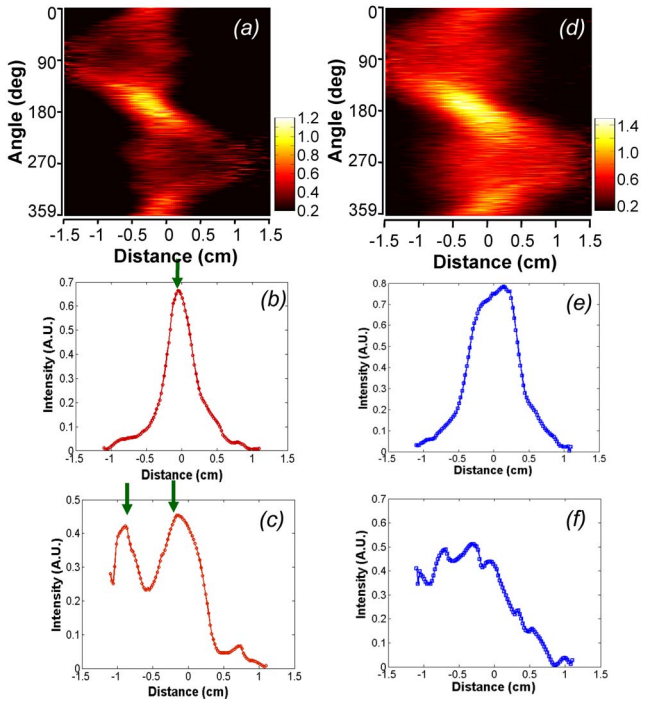

Fig. 2. (Color online) Sinograms of the transmitted normalized fluorescence intensity at each lateral position as a function of rotation angle at (a) early and (d) quasi-cw time gates. Transmitted normalized intensity profiles with the mouse oriented at 0° rotation for (b) early and (e) quasi-cw time gates as well as (c),(f) the corresponding profiles for 90° rotation are shown. See text for detailed description of temporal gates.

resulting in a negligible (~0.02 mm) difference in the photon path length. This allowed the acquisition of extremely rich data sets comprising approximately 10^4 source-detector pairs. Figures 2(c) and 2(d) show the early-photon and quasi-cw photon profiles at 0° rotation (where the tubes were approximately parallel to the laser axis). A significantly narrower fluorescent peak corresponding to the superficial tube was observed at early times versus the later gate. Similarly, Figs. 2(e) and 2(f) show the profiles at 90° rotation (where the tubes were in the center of the chamber, approximately perpendicular to the laser axis) wherein two distinct fluorescent peaks were observable with early photons, whereas these were effectively "smeared" with quasi-cw photons. The analysis of these data indicates that the FWHM of the system sensitivity function was reduced by a factor of approximately 2–3 with early photons. In summary, these projection data demonstrate the advantage of detecting early photons, since the two fluorescent tubes were significantly easier to visualize, even with individual projections.

Tomographic image reconstructions were then performed with the data. Axial slices were discretized with a 0.5 mm × 0.5 mm mesh, which was the smallest possible given MATLAB memory limitations. A vector $\boldsymbol{y}$ containing the source-detector measurements was related to the unknown fluorochrome concentration in each of the mesh nodes, described by a vector $\boldsymbol{x}$, using a matrix equation $\boldsymbol{y}=\boldsymbol{W}\cdot\boldsymbol{x}$, where $\boldsymbol{W}$ was the sensitivity matrix. In the case of early-arriving photons, $\boldsymbol{W}$ was calculated using a second-order cumulant approximation to the Boltzmann transport equation as we have done previously [8,14]. For the quasi-cw photons, $\boldsymbol{W}$ was calculated using the solution to the time-resolved diffusion equation. Matrix inversions were performed using the randomized algebraic reconstruction technique.

Figure 3 shows sample image reconstructions for early and quasi-cw photons as well as the corresponding x-ray CT images (Gamma-Medica, X-SPECT, Northridge, Calif.). Three-dimensional renderings of CT data were performed with the Amira (Mercury-TGS, Chelmsford, Mass.) and Image-J software packages. The relative rotation angle of the mouse between modalities was corrected by comparing the position of the holder rods in each. The reconstructions performed with early photons [Figs. 3(b) and 3(e)] show excellent agreement with the x-ray CT images, whereas the individual tubes were not well separated with quasi-cw reconstructions. The upper central tube in the early-photon image was slightly elongated, possibly due to the presence of outer tube. The analysis of the fluorescence images showed that based on the FWHM of the reconstructed tubes, early-photon images yielded significantly better estimates of the size versus quasi-cw photon images (true inner area=1.3 mm^2, early photon=2.1 mm^2, and quasi-cw photons=4.1 mm^2). This overestimation of the tube area was at least partly due to the finite mesh size, since tubes overlapped several grid points. While the center-to-center separation of the tubes was correctly reconstructed

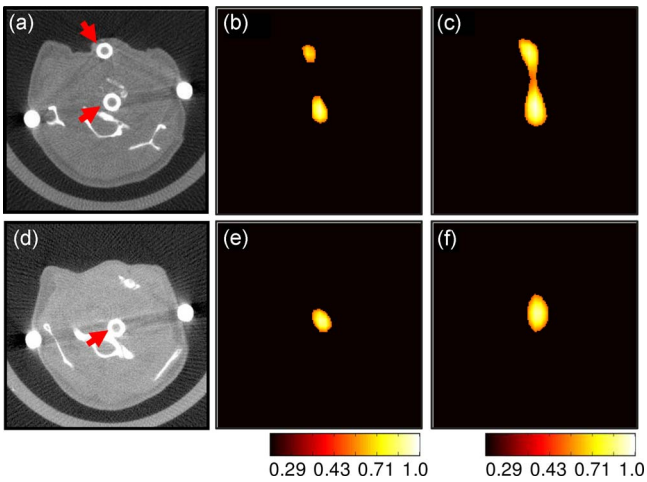

Fig. 3. (Color online) (a),(d) X-ray computed tomography images of two axial slices through the torso of the animal, indicating the location of the implanted tubes (arrows) as well as the corresponding normalized reconstructed fluorescence tomographic images for (b),(e) early-arriving and (c),(f) quasi-cw time gates. The upper slice (a)–(c) corresponds to the data from Fig. 2 where both tubes were present, whereas in the lower slice (d)–(f) only the longer central tube was visible. A display threshold of 50% of the maximum reconstructed intensity was applied to each image.

as 6 mm for both the early and quasi-cw photons, the edge-to-edge separation was more accurately reconstructed with early photons (true separation = 4 mm edge-to-edge, early photons = 3 mm, and quasi-cw = 0 mm). Recently, LeBlond *et al.* [7] showed a similar improvement with early photons using simulated data from a photomultiplier-tube-based system, although there were significant differences in the instrument design, particularly with respect to the number of source-detector pairs used in image reconstructions.

We note that the quasi-cw experimental conditions used herein were not equivalent to conventional cw FMT [1,2], since in this analysis only data points in narrow detection angles directly opposite the source positions were included, whereas in conventional FMT larger data sets are generally used. The current experiments were designed so that a direct comparison (particularly when viewing the data in Fig. 2) was possible, thereby demonstrating the value of detection of early photons in small animal imaging. It is further important to note in this case that the detected early photons were not "ballistic," since they have undergone multiple scattering events; as we have demonstrated they are nevertheless significantly less diffuse than the later-arriving quasi-cw photons. In practice, this means that accurate models of photon propagation at early times are necessary for tomographic image reconstructions. Under our experimental conditions, we have determined that the time-resolved diffusion equation is not adequate for describing photon propagation and that higher-order approximations to the Boltzmann transport equation were required. Finally, since the thoracic cavity exhibits a particularly high degree of scatter, we anticipate that an even greater improvement may be observed when imaging other organs with this technique.

This research was supported in part by the National Institutes of Health (NIH) grant R01 EB000750. The authors wish to thank Mr. Joshua Dunham and Mr. Gregory Wojtkiewicz for assistance in the experiments.

References

1. V. Ntziachristos, C. Bremer, E. E. Graves, J. Ripoll, and R. Weissleder, Mol. Imaging **1**, 82 (2002).
2. E. E. Graves, J. Ripoll, R. Weissleder, and V. Ntziachristos, Med. Phys. **30**, 901 (2003).
3. A. H. Hielscher, A. Y. Bluestone, G. S. Abdoulaev, A. D. Klose, J. Lasker, M. Stewart, U. Netz, and J. Beuthan, Dis. Markers **18**, 313 (2002).
4. G. M. Turner, A. Soubret, and V. Ntziachristos, Med. Phys. **34**, 1405 (2007).
5. J. Wu, L. Perelman, R. R. Dasari, and M. S. Feld, Proc. Natl. Acad. Sci. USA **94**, 8783 (1997).
6. W. Cai, B. B. Das, F. Liu, M. Zevallos, M. Lax, and R. R. Alfano, Proc. Natl. Acad. Sci. USA **93**, 13561 (1996).
7. F. Leblond, H. Dehghani, D. Kepshire, and B. W. Pogue, J. Opt. Soc. Am. A **26**, 1444 (2009).
8. M. J. Niedre, R. H. de Kleine, E. Aikawa, D. G. Kirsch, R. Weissleder, and V. Ntziachristos, Proc. Natl. Acad. Sci. USA **105**, 19126 (2008).
9. A. Soubret and V. Ntziachristos, Phys. Med. Biol. **51**, 3983 (2006).
10. M. J. Niedre, G. M. Turner, and V. Ntziachristos, J. Biomed. Opt. **11**, 064017 (2006).
11. B. W. Pogue and M. S. Patterson, J. Biomed. Opt. **11**, 041102 (2006).
12. N. Deliolanis, T. Lasser, D. Hyde, A. Soubret, J. Ripoll, and V. Ntziachristos, Opt. Lett. **32**, 382 (2007).
13. A. Soubret, J. Ripoll, and V. Ntziachristos, IEEE Trans. Med. Imaging **24**, 1377 (2005).
14. M. Xu, W. Cai, M. Lax, and R. R. Alfano, Phys. Rev. E **65**, 066609 (2002).